

Reconfigurable Antennas For MIMO Ad-Hoc Networks

John Kountouriotis*, Daniele Piazza*, Prathaban Mookiah*, Michele D'Amico†, Kapil R. Dandekar*

*Electrical and Computer Engineering, Drexel University, Philadelphia, PA 19104, USA

Email: {jk368, dp84, pm352, dandekar}@drexel.edu

†Electrical and Computer Engineering, Politecnico di Milano, Milano, 20133, Italy

Email: {damico}@elet.polimi.it

Abstract—In this paper we investigate the performance of reconfigurable antennas in an MIMO ad-hoc network. The nodes employ the multiuser waterfilling (known also as iterative waterfilling) power allocation [1], [2] method and we use network sum capacity as a performance metric. We study a centralized configuration selection scheme, which can be used as an upper bound in the sum capacity using reconfigurable antennas, as well as a simple distributed configuration selection scheme, suitable for use in an ad-hoc MIMO network.

I. INTRODUCTION

Reconfigurable antennas have lately drawn a lot of attention due to the promise of increased capacity in Multiple Input Multiple Output (MIMO) communications. Reconfigurable antennas have the ability to dynamically modify their radiation patterns in response to changes in the wireless propagation channel. They are ideally suited for MIMO due to the “pattern diversity” [3] they provide. To date, the increase in capacity by using reconfigurable antennas has been studied in the case of a single link (i.e. in an interference free environment) [3]–[6]. It is our belief that there is a lot of potential in using reconfigurable antennas in a MIMO ad-hoc network. In a network scenario, the configuration selection of a single link will not only aim to find the configuration combination (the configuration at the receiver and the configuration at the transmitter) that will provide a “rich” channel between the receiver and the transmitter of that link, but will also aim to mitigate the interference that the link is suffering from. We chose to consider a MIMO ad-hoc network that uses the multiuser (or iterative) waterfilling power allocation that was proposed in [1].

II. RECONFIGURABLE PRINTED DIPOLE ARRAY

The Reconfigurable Printed Dipole Array (RPDA), first introduced by the authors in [4], consists of two microstrip dipoles with variable electrical length separated by a quarter wavelength. The RPDA was characterized in single link MIMO systems through field measurements and simulations [4]. Each active element of the array can be reconfigured in length using PIN diode switches. Two configurations are possible for each dipole. Specifically, “short” and “long” configurations are defined, which corresponds to both switches being off and on respectively. Therefore four different configurations can be defined for the RPDA: both antennas “long” (l-l), both antennas “short” (s-s), one antenna “short” and the

other “long” (s-l) and vice versa (l-s). A schematic of the structure of the RPDA is depicted in Fig. 1.

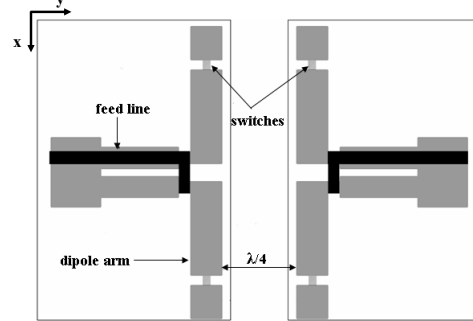


Fig. 1. Schematic of the Reconfigurable Printed Dipoles Array (RDPA).

The array is designed to work in the frequency band between 2.4 GHz and 2.48 GHz and is matched for this range of frequencies. Note then the “short” configuration performs better than the “long” configuration in terms of radiation efficiency, η (“long” configuration $\eta = 62\%$, “short” configuration $\eta = 75\%$).

The setting of the switches results in different geometries of the antenna and, consequently, in different levels of inter-element mutual coupling and array far-field radiation patterns.

The level of diversity between the patterns generated at the same port for different configurations of the array, is estimated through the spatial correlation coefficient value [7], [8]. Assuming a rich scattering environment, the spatial correlation coefficient, $\rho_{j,k,l,m}$, is defined as [8]:

$$\rho_{j,k,l,m} = \frac{\int_{4\pi} E_{j,k}(\Omega) E_{l,m}^*(\Omega) d\Omega}{[\int_{4\pi} |E_{j,k}(\Omega)|^2 d\Omega \int_{4\pi} |E_{l,m}(\Omega)|^2 d\Omega]^{1/2}} \quad (1)$$

where j and l define the array port and k and m the antenna configuration at port j and l respectively. $E_{j,k}(\Omega)$ is the radiation pattern of configuration k at port j over the solid angle $\Omega = (\phi, \theta)$ and $(*)$ is the conjugation operator. Table I reports the values of correlation between azimuthal patterns generated at the same port for all the array configurations, which can be viewed as a metric of the difference (diversity) between the two possible radiation patterns.

III. SYSTEM MODEL AND ASSUMPTIONS

We assume a flat fading channel and a network of $\mathcal{L} = [1, \dots, L]$ links (i.e. there are $2 \times L$ nodes in the network) that

TABLE I
RPDA PATTERN SPATIAL CORRELATION

	$E_{1,s-s}$	$E_{1,l-s}$	$E_{1,s-l}$	$E_{1,l-l}$
$E_{1,s-s}$	1	0.98	0.92	0.98
$E_{1,l-s}$	0.98	1	0.91	0.96
$E_{1,s-l}$	0.92	0.91	1	0.94
$E_{1,s-l}$	0.98	0.96	0.94	1

operate at the same time. $\mathbf{H}_{i_{rc},j_{tc}}$ denotes the channel between the receiver of link i and the transmitter of link j . i and j are indexed by the receive and transmit configurations, i_{rc} and j_{tc} , respectively, where $i_{rc}, j_{tc} \in [1, 4] \forall l \in \mathcal{L}$. \mathbf{x}_i is the signal vector of link i , which results in the power covariance matrix of link i , \mathbf{Q}_i as $\mathbf{Q}_i = E\{\mathbf{x}_i \mathbf{x}_i^H\}$. Operation $(\cdot)^H$ denotes the conjugate transpose. We can write the input-output relationship for link l as:

$$\mathbf{y}_l = \mathbf{H}_{l_{rc},l_{tc}} \mathbf{x}_l + \sum_{i \in \mathcal{L} \setminus l} \mathbf{H}_{l_{rc},i_{tc}} \mathbf{x}_i + \mathbf{n} \quad (2)$$

where $\sum_{i \in \mathcal{L} \setminus l} \mathbf{H}_{l_{rc},i_{tc}} \mathbf{x}_i + \mathbf{n}$ is the interference plus noise, which results in an interference plus noise covariance matrix of l : $\mathbf{R}_l = \mathbf{I} + \sum_{i \in \mathcal{L} \setminus l} \mathbf{H}_{l_{rc},i_{tc}} \mathbf{Q}_i \mathbf{H}_{l_{rc},i_{tc}}^H$. We assume that the noise has a covariance matrix equal to the identity matrix. Vector \mathbf{c} is an $1 \times 2\mathcal{L}$ vector that holds the configurations for all links, i.e. $\mathbf{c} = [1_{rc}, 1_{tc}, 2_{rc}, 2_{tc}, \dots, L_{rc}, L_{tc}]$.

IV. MULTIUSER WATERFILLING POWER ALLOCATION

Since we are investigating an ad-hoc network, we do not assume any cooperation among the different links, so each link will not take into account the interference it is imposing on the others. From this “network” perspective the performance metric of interest is the *sum* capacity of all the link in the network.

When a link undergoes interference, with interference plus noise covariance matrix \mathbf{R}_l , it has been proven [9] that the optimum power allocation is to perform waterfilling on the whitened channel matrix $\mathbf{H}_{w_l,l} = \mathbf{R}_l^{-1/2} \mathbf{H}_{l,l}$,

A change in the power allocation matrix of a single link will change the interference plus noise covariance matrix (and whitened channel matrix) of the other links. The links respond to this change by performing waterfilling on the new whitened channel matrix and the procedure converges when the whitened channel matrices remain practically unchanged [1], [2]. We assume that each link l can estimate $\mathbf{H}_{l_{rc},l_{tc}}$ as well as estimate \mathbf{R}_l for all available configurations.

A. Centralized Approach

In the case where a centralized controller exists in the network, we exhaustively perform multiuser waterfilling with every possible antenna configuration for every node in the network. Even though multiuser waterfilling is by construction a selfish procedure where each link looks after its own interest (capacity), the central controller, even indirectly, will find a solution closer to the common good (sum capacity). Mathematically, we can describe the centralized approach as:

$$\max_{\mathbf{c}} \left(\sum_{l \in \mathcal{L}} \log_2 (\det(\mathbf{I} + \mathbf{H}_{l_{rc},l_{tc}} \mathbf{Q}_l \mathbf{H}_{l_{rc},l_{tc}}^H \mathbf{R}_l^{-1})) \right) \quad (3)$$

Subject to: $Tr\{\mathbf{Q}_l\} = P_T \forall l \in \mathcal{L}$

where \mathbf{Q}_l is the power covariance matrix employed by link l that results from waterfilling on the whitened channel matrix (convergence has been reached) and \mathbf{c} is the $1 \times 2\mathcal{L}$ vector containing the antenna configurations of the links.

B. Distributed Approach

In the case where a central controller does not exist, the configuration selection will have to happen in a distributed way. What we propose is to modify multiuser waterfilling so that in each step the link will not only perform waterfilling on the whitened channel, but will also find the receive and transmit configuration that provides the most capacity achieving whitened channel (i.e. the one with the highest singular values). In order for this scheme to work, we have to make the assumption that the links can estimate the interference plus noise covariance matrix for all available receive configurations at each iteration. We also assume that each link can estimate the channel between the receiver and transmitter for all configuration combinations. Furthermore, we have to assume that the channels will not change until the algorithm converges. If we denote $\sigma_{k_{l_{rc},tc}}$ as the k^{th} singular value of link l whitened channel matrix when link l employs receive configuration rc and transmit configuration tc , then each link solves the following:

$$\max_{rc,tc} \sum_{k=1}^{\min\{N_T, N_R\}} \log_2 \left(1 + \sigma_{k_{l_{rc},tc}}^2 \left(\mu - \frac{1}{\sigma_{k_{l_{rc},tc}}^2} \right)^+ \right) \quad (4)$$

where $(x)^+ = \max\{0, x\}$ and μ is calculated so that it will satisfy the available transmit power constraint,

$\sum_{k=1}^{\min\{N_T, N_R\}} (\mu - \frac{1}{\sigma_{k_{l_{rc},tc}}^2})^+ = P_T$. The singular values of the whitened channel matrix for link l are a function of the receive and transmit configurations of link l , and the transmit configuration and power allocation of all the other links. Since link l has control only of its own configurations, it will try to find the configurations that will maximize its capacity, given the other links transmit configuration and power covariance matrices.

By comparing the resulting sum network capacity of this distributed scheme with the one resulting from the centralized scheme, we see how much we are losing when each node acts “selfishly”.

V. SIMULATIONS

The performance that can be achieved, in terms of sum network capacity, combining reconfigurable antennas and power allocation methods in MIMO ad hoc networks, according to the scheme described in Section IV, was investigated through computational electromagnetic simulations in an indoor environment.

Three different networks topologies, depicted in Fig. 2, were analyzed. Each network was composed of three transmitting nodes and three receiving nodes for a total of three 2×2 MIMO links. Six different link combinations per network topology were considered connecting each transmitter with all the receivers. Note that while topology with symbol \triangle consists

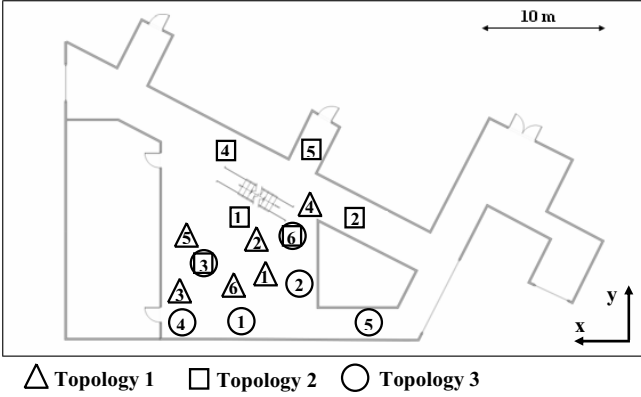


Fig. 2. Network topologies analyzed in the indoor environment. Transmitters are $\{1, 2, 3\}$ and receivers are $\{4, 5, 6\}$. Different symbols denote different topologies.

of only LOS (Line Of Sight) links, topologies denoted with \square and \bigcirc are characterized by both LOS and NLOS (Non Line Of Sight) links. Each network topology was analyzed using the reconfigurable antennas described in Section II. For every network topology, four different scenarios using reconfigurable antennas usage were investigated:

- Reconfigurable antennas at both transmitting (TX) and receiving (RX) nodes (Double Side Reconfigurable Antennas - DSRA).
- Reconfigurable antennas only at the TX (Transmit-only Reconfigurable Array - TXRA).
- Reconfigurable antennas only at the RX (Receive-only Reconfigurable Array - RXRA).
- Non-Reconfigurable antennas at both TX and RX.

For the case when non-reconfigurable antennas are used, the most efficient (in terms of radiation efficiency) antenna configuration of the RPDA is chosen as the non-reconfigurable antenna (“short-short” configuration). The motivation for using reconfigurable antennas at one link end is because of lower complexity.

The channels in the network were determined via numerical computation using an electromagnetic ray tracer, FASANT [10]. A 3D model of the hallway of the 3rd floor of the Bossone Research building on Drexel University campus was simulated as the geometry input of FASANT. Radiation patterns for the RDPA in all configurations were obtained using FEKO, an antenna design software based on the method of moments (MoM) [11].

Each of the three network topologies, depicted in Fig. 2, was simulated. Both the transmitting and receiving nodes were located at a height of 1.5 m. For each receiver location the node was moved on a 10×10 grid of points (100 points) separated by 0.03λ in order to provide local averaging and simulate the small scale effects of the wireless channel.

The simulations were conducted by transmitting a single tone at 2.484 GHz to obtain the entries of the channel matrices, \mathbf{H} , for each link of interest and for each interfering link. The extracted channel matrices were then used to calculate the sum network capacity (i.e., the objective of equation 3) for the

techniques described in Section IV.

VI. RESULTS

For the results presented in this section, an available transmit power per link of 20 dB was used. The stopping criteria for the centralized approach was similar to one used in [2]. The iteration was assumed to have converged when the maximum change in any power allocation matrix $\mathbf{Q}_i, i \in \mathcal{L}$ did not exceed 10^{-3} . For the distributed scheme, on top of the requirement for the power allocation matrices change, the iterations should go on if there is any switching in the array configuration. In all cases, both centralized and distributed, a maximum of 200 iterations was allowed before concluding that the iterations do not converge.

A. Centralized Scheme

In figure 3 the empirical cdfs of the sum network capacity are plotted for the 3 centralized schemes (DSRA, TXRA and RXRA) we investigated. In the same plot, the empirical cdf for the case of non-reconfigurable antennas is plotted for comparison. The cdf plots are “intuitive”, in the sense that the best performance is achieved by the DSRA scheme, while the two single sided schemes perform close to each other and each achieve almost half of the improvement that the DSRA shows. The TXRA scheme performs better than RXRA, which can also be verified by Table II, where the expected sum network capacities and the percentage increase as compared to the non-reconfigurable case appear. From this table we can also verify that the performance increase (in terms of sum capacity) that we can achieve by using RDPA in a MIMO ad hoc network is significant and can be as high as 27% for the DSRA. For the single side schemes the improvement is almost 18% for the TXRA and around 12% for the RXRA.

B. Distributed Scheme

The empirical cdfs of the sum network capacity for the proposed distributed scheme appear in figure 4 together with the non-reconfigurable case. As is evident, there are significant changes when compared with the trends of the centralized scheme. First of all, we can see that the distributed TXRA scheme performs rather poorly, since it is very close to the cdf plot of the non-reconfigurable case. From Table II we can see that the improvement from the TXRA scheme is only around 2%. This result occurs because most amount of time, the links chose their transmit configurations to be the same as the non-reconfigurable case, which are the most power efficient. Thus, the objective that each link has to maximize its own capacity leads to transmit configurations that cause a great amount of interference to other links and thus bring the sum capacity down.

The most important thing to notice in figure 4 is that the cdfs of DSRA and RXRA fall almost on top of each other and by looking at table II we can see that the percentage improvement for the RXRA (9.5%) scheme is slightly higher than the one that the DSRA (9.17%) achieves. So, the freedom that the links had to jointly choose their transmit and receive configurations (DSRA scheme) actually led to a

TABLE II
SUM NETWORK CAPACITY COMPARISON

	Mean Value	Percentage Increase
DSRA - Centr.	12.8255	27.92%
RXRA - Centr.	11.2539	12.25%
TXRA - Centr.	11.8269	17.96%
DSRA - Distr.	10.9455	9.17%
RXRA - Distr.	10.9776	9.5%
RXRA - Distr.	10.2457	2.19%
Non-Reconfigurable	10.0259	0%

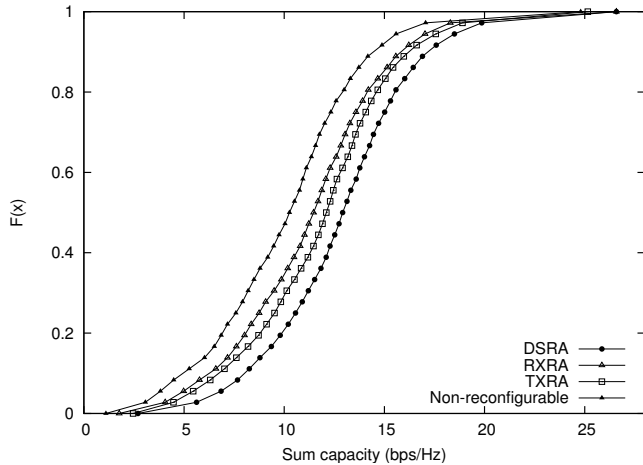


Fig. 3. Centralized scheme empirical sum network capacity CDFs

worse solution than the transmit configuration is fixed and the receive configuration is reconfigurable (RXRA scheme). This result can be attributed to the nature of the distributed approach, where each link acts selfishly in its own interest. Specifically, as we have seen in section VI-A, when (even indirect) cooperation among the nodes is imposed, the freedom to choose transmit configurations more greatly benefits both DSRA and TXRA schemes.

The convergence properties of the original multiuser waterfilling technique did not seem to change with the proposed extension to incorporate the antenna configuration selection. For both the centralized (which is in essence the original multiuser waterfilling) and distributed approaches the iterations converged for more than 99% of the time, while for all cases around 6-7 iterations were needed.

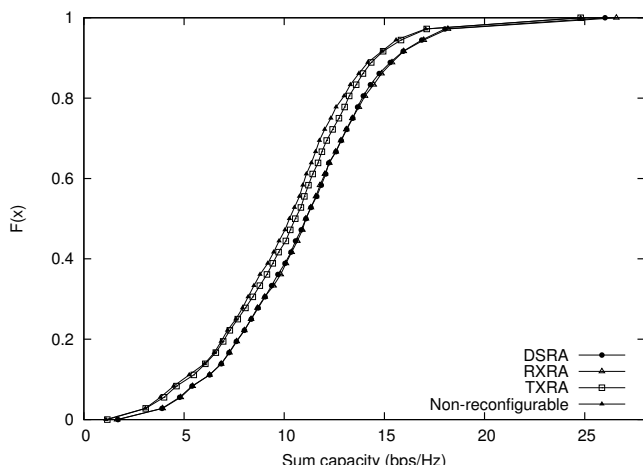


Fig. 4. Distributed scheme empirical sum network capacity CDFs

VII. CONCLUSIONS

In this work we have seen what kind of performance increase can be expected (in terms of sum capacity) in a MIMO ad-hoc network when reconfigurable RDPA are used. We have investigated a centralized approach that was used as an upper bound metric on the performance increase and we have proposed a simple extension to the well-known multiuser waterfilling algorithm to incorporate the antenna configuration selection in the iterations. The results showed a significant amount of increase in performance when we use reconfigurable antennas as opposed to the use of conventional, non-reconfigurable ones. We have also shown that it is not really necessary to have reconfigurable antennas at both ends of the link, since we can have good results even in the case when only the receiver employs reconfigurable antennas. We expect to see more increase in performance if antennas that have more “diverse” radiation patterns between different configurations (as expressed by the quantities that appear in table I) are employed in the network, like the reconfigurable antennas that appear in [5].

ACKNOWLEDGMENTS

This material is based upon work supported by the National Science Foundation under Grants 0435041 and 0322797.

REFERENCES

- [1] M. Demirkol and M. Ingram, “Power-controlled capacity for interfering MIMO links,” *IEEE Vehicular Technology Conference*, vol. 1, no. 54D, pp. 187 – 191, 2001.
- [2] S. Ye and R. S. Blum, “Optimized signaling for MIMO interference systems with feedback,” *IEEE Transactions on Signal Processing*, vol. 51, no. 11, pp. 2839 – 2848, 2003.
- [3] A. Foreza and R. W. Heath Jr., “Benefit of pattern diversity via two-element array of circular patch antennas in indoor clustered MIMO channels,” *IEEE Transactions on Communications*, vol. 54, no. 5, pp. 943 – 954, 2006.
- [4] D. Piazza and K. Dandekar, “Reconfigurable antenna solution for MIMO-OFDM systems,” *Electronics Letters*, vol. 42, no. 8, pp. 15 – 16, 2006.
- [5] D. Piazza, P. Mookiah, M. D’Amico, and K. Dandekar, “Computational electromagnetic analysis of a reconfigurable multiport circular patch antenna for MIMO communications,” *to appear in Proceedings of the International Symposium on Electromagnetic Theory, EMTS*, 2007.
- [6] B. A. Cetiner, H. Jafarkhani, J.-Y. Qian, H. J. Yoo, A. Grau, and F. De Flaviis, “Multifunctional reconfigurable MEMS integrated antennas for adaptive MIMO systems,” *IEEE Communications Magazine*, vol. 42, no. 12, pp. 62 – 70, 2004.
- [7] C. Waldschmidt, J. Hagen, and W. Wiesbeck, “Influence and modelling of mutual coupling in MIMO and diversity systems,” *IEEE Antennas and Propagation Society, AP-S International Symposium (Digest)*, vol. 3, pp. 190 – 193, 2002.
- [8] R. Vaughan and J. Andersen, “Antenna diversity in mobile communications.” *IEEE Transactions on Vehicular Technology*, vol. T-36, no. 4, pp. 149 – 172, 1987.
- [9] F. Farrokhi, G. Foschini, A. Lozano, and R. Valenzuela, “Link-optimal BLAST processing with multiple-access interference,” *IEEE Vehicular Technology Conference*, vol. 1, no. 52D, pp. 87 – 91, 2000.
- [10] M. F. Catedra, J. Perez, A. Gonzalez, O. Gutierrez, and F. Saez de Adana, “Fast computer tool for the analysis of propagation in urban cells,” *Annual Wireless Communications Conference, Proceedings*, pp. 240 – 245, 1997.
- [11] D. B. Davidson, I. P. Theron, U. Jakobus, F. M. Landstorfer, F. J. Meyer, J. Mostert, and J. J. van Tonder, “Recent progress on the antenna simulation program FEKO,” *Proceedings of the South African Symposium on Communications and Signal Processing, COMSIG*, pp. 427 – 430, 1998.